ChemComm

A NiRhS Fuel Cell Catalyst –Lessons from Hydrogenase

Journal:	*ChemComm*
Manuscript ID	CC-COM-07-2020-004789.R1
Article Type:	Communication

COMMUNICATION

A NiRhS Fuel Cell Catalyst –Lessons from Hydrogenase †

Seiji Ogo,*[a,b] Tatsuya Ando, [a,b] Le Tu Thi Minh, [a] Yuki Mori, [a] Takahiro Matsumoto, [a,b] Takeshi Yatabe, [a,b] Ki-Seok Yoon, [a,b] Yukio Sato, [c] Takashi Hibino [b,d] and Kenji Kaneko [b,c]

Received 00th January 20xx,
Accepted 00th January 20xx

DOI: 10.1039/x0xx00000x

We present a novel fuel cell heterogeneous catalyst based on rhodium, nickel and sulfur with power densities 5-28% that of platinum. The NiRhS heterogeneous catalyst was developed via a homogeneous model complex of the [NiFe]hydrogenases (H_2ases) and can act as both the cathode and anode of a fuel cell.

We have previously reported a NiRu model complex, $[Ni^{II}(X)(H_2O)(\mu\text{-}H)Ru^{II}(\eta^6\text{-}C_6Me_6)](NO_3)$ {[**3**](NO$_3$), X = *N*,*N*'-dimethyl-3,7-diazanonane-1,9-dithiolato}, that can mimic the chemical functions of O_2-tolerant [NiFe]H_2ases.[1–3] This complex is based on a central NiRu bimetallic core with flexible μ-S bridges, which allow the close approach of the two metal centres. This complex can perform both H_2-oxidation and O_2-reduction, in a similar manner to O_2-tolerant [NiFe]H_2ases,[1,3,4] and thus acts as both an anode and cathode catalyst for H_2-O_2 fuel cells.[5] However, the successful functioning of the compound did not extend as far as producing an efficient fuel cell.[5] Since organometallic catalysts are not as robust as their solid-state, heterogeneous counterparts, we investigated the possibility of using dry distillation (pyrolysis) to remove the volatile elements and leave behind the active μ-S bimetallic core. We investigated three bimetallic complexes where nickel was partnered with ruthenium, rhodium and iridium and the NiRh complex gave the best results.

Herein, we describe the synthesis, characteristics and catalytic properties of the NiRh organometallic complex before detailing its conversion into the NiRhS dry-distilled catalysts (DDCs). We then demonstrate the catalytic properties of these dry-distilled compounds and their application as the first DDCs containing two different metals and sulfur that function as both the anode and cathode of functioning fuel cells (Fig. S1, Table S1, ESI†).[6]

A $Ni^{II}Rh^{III}$ dichloride complex $[Ni^{II}Cl(X)Rh^{III}Cl(\eta^5\text{-}C_5Me_5)]$ (**1**) was prepared from the reaction of $[Ni^{II}(X)]$ with $[Rh^{III}(\eta^5\text{-}C_5Me_5)Cl_2]_2$. This water-soluble complex was then characterized by X-ray analysis (Fig. S2, Table S2, ESI†), electrospray ionization mass spectrometry (ESI-MS, Fig. S3, ESI†) and ^{1}H NMR (Fig. S4, ESI†) and IR spectroscopies (Fig. S5, ESI†). Its structure is based around a Ni(μ-S)$_2$Rh butterfly core, which is similar to our previously-reported [NiFe]H_2ase mimics.[1,7]

Having synthesized **1**, we proceeded to investigate its catalytic properties. Complex **1** activated H_2 (0.1 MPa) heterolytically in water to afford a $Ni^{II}Rh^{III}$ hydride complex $[Ni^{II}Cl(X)(\mu\text{-}H)Rh^{III}(\eta^5\text{-}C_5Me_5)]$ (**2**) in a similar manner to H_2ases (Fig. 1 and 2a).[1,3,7,8] The structure was determined by X-ray analysis (Fig. 1), UV-vis spectroscopy (Fig. S6, Tables S2 and S3, ESI†), ESI-MS (Fig. S7, ESI†) and IR spectroscopy (Fig. S8, ESI†). The X-ray analysis showed that the Ni1···Rh1 interatomic distance had been shortened to 2.7454(16) Å, with a bridging hydride ligand between the two metal centres (Fig. 1). This structural change upon the activation of H_2 and complexation of the hydride is similar to that found in our other [NiFe]H_2ase models and the natural [NiFe]H_2ases themselves.[1,7,9] The origin of the bridging hydride was derived from dihydrogen gas, as confirmed by the formation of a deuteride complex $[Ni^{II}Cl(X)(\mu\text{-}D)Rh^{III}(\eta^5\text{-}C_5Me_5)]$ (D-labelled **2**) from the treatment of **1** with D_2 (Fig. S7 and S8, ESI†).

[a] *Department of Chemistry and Biochemistry, Graduate School of Engineering, Kyushu University*
International Institute for Carbon-Neutral Energy Research (WPI-I2CNER), Kyushu University,
744 Moto-oka, Nishi-ku, Fukuoka 819-0395 (Japan)
E-mail: ogo.seiji.872@m.kyushu-u.ac.jp.
[b] *Center for Small Molecule Energy, Kyushu University, 744 Moto-oka, Nishi-ku, Fukuoka 819-0395 (Japan).*
[c] *Department of Materials Science and Engineering, Faculty of Engineering, Kyushu University, 744 Moto-oka, Nishi-ku, Fukuoka 819-0395 (Japan).*
[d] *Graduate School of Environmental Studies, Nagoya University, Furo-cho, Chikusa-ku, Nagoya 464-8601 (Japan)*

†Electronic Supplementary Information (ESI) available: [Experimental details, Table S1–S8 and Fig. S1–S21.]. CCDC 1996959 and 1996960. For ESI and crystallographic data in CIF or other electronic format see DOI: 10.1039/x0xx00000x

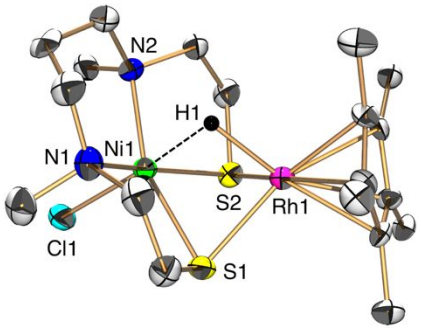

Fig. 1 ORTEP drawing of **2** with ellipsoids set at the 50% probability level. The hydrogen atoms of the ligand X (*N*,*N*′-dimethyl-3,7-diazanonane-1,9-dithiolato) and C_5Me_5 are omitted for clarity. Selected interatomic distances [Å] and angles [°]: Ni1···Rh1 2.7454(16), Rh1–H1 1.84(9), Ni1–H1 1.96(9), Ni1–S1–Rh1 71.15(7), Ni1–S2–Rh1 70.65(7) for **2**.

We then investigated the catalytic properties of **1** by using 2,6-dichlorobenzeneindophenol (DCIP) as an acceptor of $2e^-$ and $2H^+$ under stoichiometric conditions with **2** and catalytic conditions with **1** (Eq. (1)). Under stoichiometric conditions (**2** : DCIP = 1 : 1) in the absence of H_2 in water, **2** is capable of reducing DCIP to $DCIPH_2$ (Fig. S9 and S10, Table S3, ESI†). Under catalytic conditions (**1** : DCIP = 1 : 27) in the presence of H_2 in water (buffer solution), H_2 reduces DCIP to $DCIPH_2$ with the assistance of **1** (Fig. 2a). The catalytic reaction is pH-dependent (Fig. S11, Table S4, ESI†) and it shows a maximum turnover number (TON) value of 14.3–15.2 at pH 4.0–5.0 (TON, mol of $DCIPH_2$/mol of **1**), similar to our previously-reported system.[4]

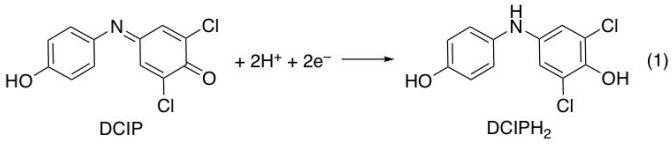

The hydride complex **2** can also reduce O_2 to H_2O (Fig. 2b, Fig. S12, Table S3, ESI†). The O_2-reduction in water was confirmed by an $^{18}O_2$-experiment wherein $H_2{}^{18}O$ was formed from the reaction of **2** with $^{18}O_2$, as observed by gas chromatography mass spectrometry (GC-MS). The TON value (TON, [(mol of $H_2{}^{18}O$)/(mol of **1**)]/2) was determined to be 0.48 in the reaction using **1** with H_2 as an electron donor (Table S4, ESI†).[10–12]

Having satisfied ourselves that the NiRh catalyst was a successful analogue of our NiRu catalyst, we set about rendering it in a heterogeneous, solid-state form. To achieve this, we used dry distillation of **1** with carbon black, in pyrolysis experiments at 100–800 °C under vacuum (ca. 15–20 Pa).[13] Following this process, the volatile elements were removed to mainly leave Ni, Rh and S atoms. The structural properties of the resulting solids were analysed by thermogravimetry-differential scanning calorimetry (TG-DSC), X-ray photoelectron spectroscopy (XPS), elemental analysis, X-ray powder diffraction (XRD) analysis, (scanning) transmission electron microscopy ((S)TEM) and energy-dispersive X-ray spectroscopy (EDS) mapping (Table S5, ESI†).

The thermal properties of **1** were investigated by TG-DSC under an N_2 atmosphere (Fig. 3, Fig. S13, ESI†). Weight loss began around 250 °C and was mostly completed by about 400–450 °C. Some endothermic peaks in the process suggest vaporization of decomposed products that should mainly contain Cl, H and N atoms, as detailed below.

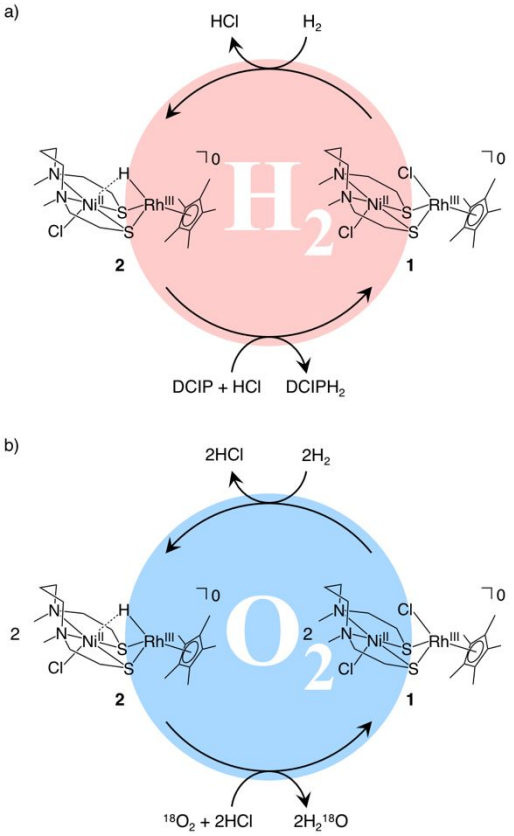

Fig. 2 Proposed catalytic mechanisms for a) H_2-oxidation and b) O_2-reduction with NiRh complexes in water. DCIP: 2,6-dichlorobenzeneindophenol. $DCIPH_2$: reduced-form of DCIP.

XPS measurements also show that the structural change of **1** depends on the temperature of dry distillation (Fig. S14, ESI†). Above 300 °C, the binding energies at 162.3–163.6 eV for S $2p_{3/2}$, 307.4–307.8 eV for Rh $3d_{5/2}$ and 853.0 eV for Ni $2p_{3/2}$ are observed in XP spectra, which might be derived from metal sulfides coexisting with Rh^0.[6c,14,15]

XRD analysis also indicates transformation of **1** to DDCs depending on the dry distillation temperatures (Fig. S15, ESI†). Complex **1** should change to DDCs at 200–300 °C and then DDCs further could be structurally changed at 700–800 °C. The XRD patterns of DDCs prepared at 300–700 °C seem to be similar to those of $Rh_{17}S_{15}$ and Rh_3S_4,[15] but not completely correspond to them. The DDC prepared at 800 °C might be attributed to S-doped NiRh alloy.[14b]

Elemental analyses were performed to determine the ratios of C : H : N : S, according to the heating temperatures (Fig. 3, Table S6, ESI†). The ratio of N decreased from 2.30% to only 0.25% upon raising the heating temperature from 200 °C to 300 °C, with a similar trend for H (Table S6, ESI†). These profiles are

almost the same as the TG curve shown in Fig. 3 and strongly indicate that the weight loss at 200–300 °C is caused by vaporization of N- and H-containing fragments. S, however, only deceased from 5.36% to 3.88%, even after heating to 800 °C, indicating that the DDCs bear significant amounts of this element.

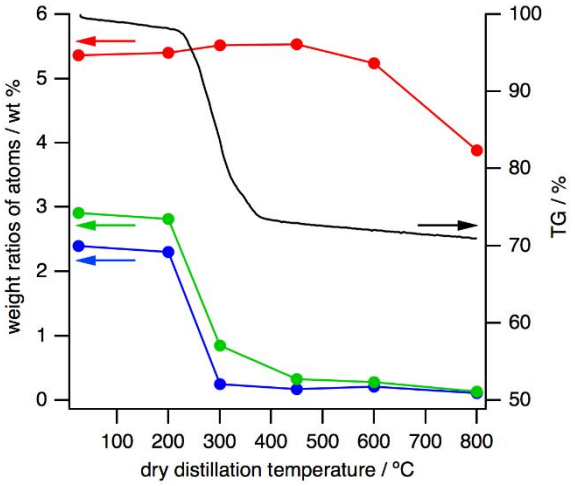

Fig. 3 A TG curve obtained from TG-DSC analysis of mixture of **1** and carbon black (1:1 weight ratio) (black line), and dry distillation temperature-dependent ratios of S (red line), N (blue line) and H (green line) atoms in DDCs determined by elemental analysis. At the point of 25 °C, mixture of **1** and carbon black (1:1 weight ratio) is used, i.e. no dry distillation.

Bright-field (BF-)TEM, annular dark field (ADF-)STEM and STEM-EDS analyses were conducted to analyse the particle form and elemental distribution in the DDCs (Fig. 4, Fig. S16, ESI†). At the heating temperatures above 200 °C, nanoparticles with a particle size of 50 nm or less were formed. Elemental mapping reveals that Ni, Rh and S atoms are distributed homogeneously under 280 °C but inhomogeneously above 300 °C.

Based on these results, we conclude that the homogeneous $Ni^{II}(\mu\text{-}S)_2Rh^{III}$ catalyst is converted into heterogeneous NiRhS-based catalysts by loss of N, H and Cl atoms at 300–600 °C, with a slight loss of S atoms at 800 °C.[15]

To examine the catalytic activities of DDCs, H_2-oxidation and $^{18}O_2$-reduction are investigated in flask experiments. The DDCs are able to remember the reactivity of **1** to catalytically oxidize H_2 and reduce $^{18}O_2$. The composition of NiRhS should remind us of [NiFe]H_2ases. The TON values of H_2-oxidation and $^{18}O_2$-reduction are increased to 4.3 and 3.5 times higher than those of **1**, respectively, by dry distillation (Tables S4 and S7, ESI†).

Following the successful enhancement of catalytic activities by dry distillation, we assembled polymer electrolyte fuel cells (PEFCs) with **1** or DDCs as anode and/or cathode catalysts (Fig. S17, ESI†). A membrane electrode assembly (MEA) with Nafion membrane was made in the same way as molecular fuel cells.[5,16]

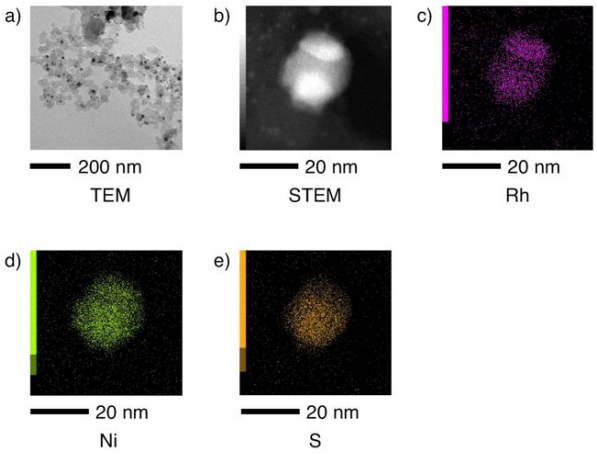

Fig. 4 a) BF-TEM image, b) ADF-STEM image and STEM-EDS elemental mappings of c) Rh, d) Ni and e) S of the dry-distilled catalyst (DDC) prepared at 600 °C.

The dependence of maximum power densities on dry distillation temperatures was investigated with DDCs as electrode catalysts for either the anode or the cathode (Fig. 5, Fig. S18 and S19, Tables S4 and S8, ESI†). The maximum power densities and open circuit voltages (OCVs) obtained where DDCs were employed as the anode and Pt/C as the cathode, were significantly enhanced above 300 °C (Fig. 5a). The highest maximum power density of 4.85 mW cm^{-2} and OCV of 1.00 V were obtained by using the DDC prepared at 600 °C (Fig. 5a, Fig. S18, Table S8, ESI†). This maximum power density is 164 times higher than that of precursor **1** and nearly 5% of that of Pt. Thereafter, the same catalysts were applied as the cathode to fabricate and evaluate PEFCs. As before, performances drastically enhanced above the dry distillation temperature of 300 °C, with the DDC prepared at 600 °C exhibiting the best performance with an OCV of 0.78 V and a maximum power density of 26.1 mW cm^{-2}, which is 28% of that of Pt (Fig. 5b, Fig. S19, Table S8, ESI†). This power density is 139 times higher than that of **1**.[17]

Electrochemical aspects for H_2-oxidation and O_2-reduction with **1** and the DDC prepared at 600 °C were investigated by means of Tafel plots and impedance spectra (Fig. S20 and S21, Table S9, ESI†). Exchange current densities of 0.0286 mA cm^{-2} and 0.0161 mA cm^{-2} were estimated for H_2-oxidation and O_2-reduction with **1**, respectively, by Tafel plots (Fig. S20, Table S9, ESI†), which are slightly lower than those of our previously-reported $Ni^{II}Ru^{II}$ complex.[18] The exchange current densities can drastically increase by dry distillation, as determined to be 13.9 mA cm^{-2} for H_2-oxidation and 10.5 mA cm^{-2} for O_2-reduction, respectively, by using the DDC prepared at 600 °C (Fig. S20, ESI†). It means the DDC has higher charge-transfer ability on electrode. In impedance spectra, no Warburg impedances were observed for the DDC, which indicates fast gas diffusion and rapid dissociative adsorption, different from **1** (Fig. S21, ESI†).

Finally, we investigated the characteristics of a fuel cell using the DDCs prepared at 600 °C as both the anode and the cathode (Fig. S22b, Tables S4 and S8, ESI†). The fuel cell generated an OCV of 0.78 V and a maximum power density of 4.53 mW cm^{-2},

a 449-fold improvement in maximum power density over **1** as catalysts for both electrodes (Fig. S22, ESI†).

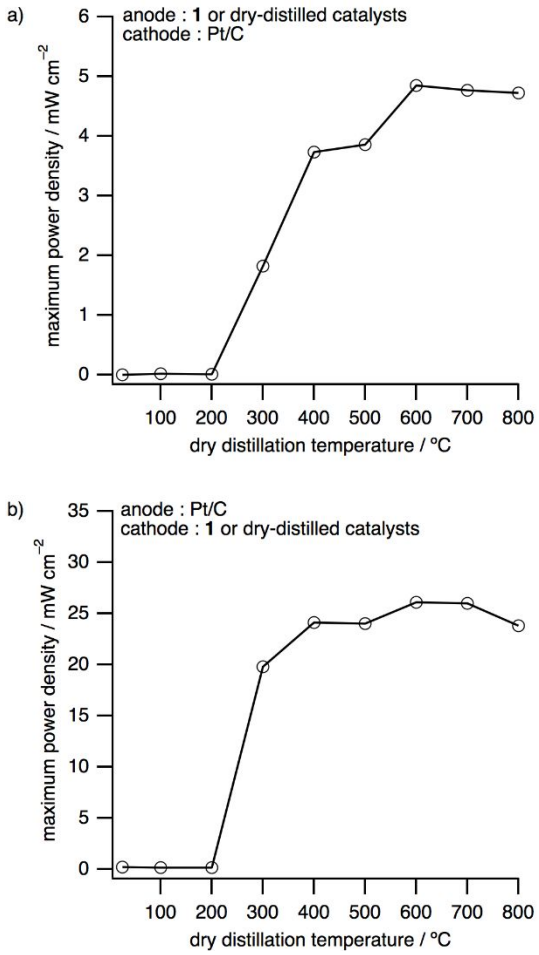

Fig. 5 Maximum power densities of H_2-O_2 fuel cells depending on dry distillation temperatures. At the dry distillation temperature of 25 °C, **1** is used as it is for a fuel cell catalyst. a) Anode: **1** or DDCs. Cathode: Pt/C. b) Anode: Pt/C. Cathode: **1** or DDCs.

In this paper, we have shown that a Rh analogue of our previous [NiFe]H_2ase models successfully functions in a similar manner. Crucially, however, we have been able to transform it by dry distillation into heterogeneous catalysts with maximum power densities nearly 5–28% of that of platinum. While these new catalysts fall short of the performance of platinum, they point the way towards linking the stepwise development of new, heterogeneous, fuel cell catalysts with the development of homogeneous organometallic catalysts.

This work was supported by JST CREST Grant Number JPMJCR18R2, Japan, JSPS KAKENHI Grant Numbers JP26000008 (Specially Promoted Research), JP18H02091, JP19K05503 and the World Premier International Research Center Initiative (WPI), Japan.

Conflicts of interest

There are no conflicts to declare.

Notes and references

1 (a) S. Ogo, R. Kabe, K. Uehara, B. Kure, T. Nishimura, S. C. Menon, R. Harada, S. Fukuzumi, Y. Higuchi, T. Ohhara, T. Tamada and R. Kuroki, *Science*, 2007, **316**, 585; (b) S. Ogo, *Coord. Chem. Rev*., 2017, **334**, 43.
2 (a) X. Yang, L. C. Elrod, J. H. Reibenspies, M. B. Hall and M. Y. Darensbourg, *Chem. Sci*., 2019, **10**, 1368; (b) C. Wombwell, C. A. Caputo and E. Reisner, *Acc. Chem. Res*., 2015, **48**, 2858.
3 W. Lubitz, H. Ogata, O. Rüdiger and E. Reijerse, *Chem. Rev*., 2014, **114**, 4081.
4 (a) T. Matsumoto, B. Kure and S. Ogo, *Chem. Lett.*, 2008, **37**, 970; (b) T. Matsumoto, T. Ando, Y. Mori, T. Yatabe, H. Nakai and S. Ogo, *J. Organomet. Chem*., 2015, **796**, 73.
5 T. Matsumoto, K. Kim and S. Ogo, *Angew. Chem. Int. Ed.*, 2011, **50**, 11202.
6 (a) N. Singh, M. Gordon, H. Metiu and E. McFarland, *J. Appl. Electrochem.*, 2016, **46**, 497; (b) Y. Shimizu, S. Yamamoto and M. Ono, *Jpn. Kokai Tokkyo Koho* 2007, JP 200787827; (c) B. Chen, G. Ma, Y. Zhu, J. Wang, W. Xiong and Y. Xia, *J. Power Sources*, 2016, **334**, 112; (d) Y. Li and T. V. Nguyen, *J. Power Sources*, 2018, **382**, 152; (e) R. W. Reeve, P. A. Christensen, A. J. Dickinson, A. Hamnett and K. Scott, *Electrochim. Acta*, 2000, **45**, 4237; (f) M. Shen, C. Ruan, Y. Chen, C. Jiang, K. Ai and L. Lu, *ACS Appl. Mater. Interfaces*, 2015, **7**, 1207; (g) F. Wang, P. Zhang, S. You, J. Du, B. Jiang, X. Li, Z. Cai, N. Ren and J. Zou, *J. Colloid Interface Sci*., 2020, **567**, 65; (h) Y. Sun, Y. Dai, Y. Duan, X. Xu, Y. Lv, L. Yang and J. Zou, *Carbon*, 2017, **119**, 394; (i) D. Guo, S. Han, R. Mac, Y. Zhou, Q. Liu, J. Wang and Y. Zhu, *Microporous Mesoporous Mater*., 2018, **270**, 1; (j) P. Chandran, A. Ghosh and S. Ramaprabhu, *Sci. Rep.*, 2018, **8**, 3591; (k) F. Möller, S. Piontek, R. G. Miller and U.-P. Apfel, *Chem. Eur. J*., 2018, **24**, 1471.
7 S. Ogo, K. Ichikawa, T. Kishima, T. Matsumoto, H. Nakai, K. Kusaka and T. Ohhara, *Science*, 2013, **339**, 682.
8 (a) R. M. Bullock and M. L. Helm, *Acc. Chem. Res*., 2015, **48**, 2017; (b) B. C. Manor and T. B. Rauchfuss, *J. Am. Chem. Soc*., 2013, **135**, 11895.
9 H. Ogata, K. Nishikawa and W. Lubitz, *Nature*, 2015, **520**, 571.
10 T. Kishima, T. Matsumoto, H. Nakai, S. Hayami, T. Ohta and S. Ogo, *Angew. Chem. Int. Ed.*, 2016, **55**, 724.
11 P. Wulff, C. C. Day, F. Sargent and F. A. Armstrong, *Proc. Natl. Acad. Sci. U.S.A.*, 2014, **111**, 6606.
12 J. Fritsch, O. Lenz and B. Friedrich, *Nat. Rev. Microbiol*., 2013, **11**, 106.
13 F. A. Westerhaus, R. V. Jagadeesh, G. Wienhöfer, M.-M. Pohl, J. Radnik, A.-E. Surkus, J. Rabeah, K. Junge, H. Junge, M. Nielsen, A. Brückner and M. Beller, *Nat. Chem.*, 2013, **5**, 537.
14 (a) J. F. Moulder, W. F. Stickle, P. E. Sobol and K. D. Bomben, *Handbook of X-ray Photoelectron Spectroscopy*, Physical Electronics Inc., Minnesota, 1995; (b) J. Lu, Z. Tang, L. Luo, S. Yin, P. K. Shen and P. Tsiakaras, *Appl. Catal. B*, 2019, **255**, 117737.
15 J. Masud, T. V. Nguyen, N. Singh, E. McFarland, M. Ikenberry, K. Hohn, C.-J. Pan and B.-J. Hwang, *J. Electrochem. Soc.*, 2015, **162**, F455.
16 S. P. Annen, V. Bambagioni, M. Bevilacqua, J. Filippi, A. Marchionni, W. Oberhauser, H. Schönberg, F. Vizza, C. Bianchini and H. Grützmacher, *Angew. Chem. Int. Ed.*, 2010, **49**, 7229.
17 M. Lefèvre, J. P. Dodelet and P. Bertrand, *J. Phys. Chem. B*, 2002, **106**, 8705.
18 T. Matsumoto, K. Kim, H. Nakai, T. Hibino and S. Ogo, *ChemCatChem*, 2013, **5**, 1368.

Table of Contents Entry

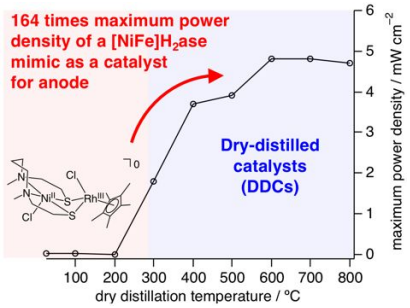

Novel dry-distilled catalysts based on Rh, Ni, and S were developed via a Ni(μ-S)$_2$Rh organometallic [NiFe]hydrogenase mimic.